Growth and morphology of Ni/Cu(100) ultrathin films: An *in situ* study using scanning tunneling microscopy

J. Shen,* J. Giergiel, and J. Kirschner
Max-Planck-Institut für Mikrostrukturphysik, Weinberg 2, D-06120 Halle/Saale, Germany
(Received 17 April 1995)

A scanning tunneling microscopy (STM) study is presented of the growth of Ni films on Cu(100). From a series of STM images taken of the same surface region during film growth, detailed information is gained on the film growth and morphology. Multilayer growth starts after nearly layer-by-layer growth of 3.5 layers, and becomes dominant above film thicknesses of 6 ML. Above 4 ML the islands are of rectangular shape, with their edges along [011] and [0$\bar{1}$1] directions. Annealing the film at a temperature of 450 K smooths the film surface without any significant substrate interdiffusion. Magneto-optical Kerr-effect measurements show the magnetization of a 10.2-ML film to remain perpendicular with a reduction less than 15% in amplitude, suggesting that the morphology is not responsible for the spin reorientation in this system.

I. INTRODUCTION

Epitaxial ultrathin films of 3*d* metals often show an interesting and striking magnetism different from that of its bulk. The reduced dimensionality and the slightly modified lattice constant owing to the pseudormorphic growth on the substrate allow the magnetic moment to be enhanced and the easy magnetization axis to run perpendicular to the surface. By varying the film preparation conditions, i.e., by different substrates, substrate temperatures or deposition rates, one can modify the structural properties in order to improve the magnetic properties of the film. This can be achieved by the knowledge of the correlation between the film magnetism and its growth, structure, and morphology. The morphology as one of the factors of the structural properties of the film is becoming increasingly important for determining the magnetism of the film. For example, in ultrathin film systems like Fe/W(110) (Ref. 1) and Fe/Cu(100),[2] the onset of the morphology percolation shows a strong correlation to the onset of ferromagnetism.

A system, which recently has attracted interest in the study of 3*d* metal ultrathin films, is Ni/Cu(100). A magneto-optical Kerr-effect (MOKE) study[3] indicates that in this system, the critical thickness for the anisotropy transition from in-plane to out-of-plane is around 7 ML. This change of the easy axis of magnetization has also been observed by x-ray magnetic circular dicroism[4] and ferromagnetic resonance[5] studies. The elucidation of the origin of the unusual transitions of anisotropy as well as dimensionality of magnetism requires the thorough investigation of the structural properties.

There are relatively few studies treating some of the structural properties of Ni/Cu(100). Under 2.5% of tensile strain in the lateral direction ($a_{Ni}=3.52$ Å, $a_{Cu}=3.61$ Å), Ni was found[3,6] to grow on Cu(100) in a layer-by-layer growth mode up to 4–5 ML. An x-ray photoelectron diffraction study[7] of a 10-ML Ni film indicated that the intraplane lattice constant of Ni films was identical to the substrate copper, resulting in a subsequently contracted interlayer distance that is very close to that of the bulk Ni. However, to the best of our knowledge, the morphology at various coverages, particularly at the thickness where the magnetic transformation occurs, is not yet known. In this paper, an ultrahigh vacuum scanning tunneling microscope (STM) is used for *in situ* study of the morphology of Ni/Cu(100) with increasing coverage at room temperature.

II. EXPERIMENTAL DETAILS

The experiment was carried out in an ultrahigh vacuum chamber (base pressure 9×10^{-9} Pa) equipped with STM, cylindrical mirror analyzer based Auger electron spectroscopy (AES), and MOKE. The copper substrate was initially prepared by 1-keV Ar^+ sputtering at room temperature until AES did not show any contamination, followed by a 500-eV sputtering at 600 °C for 2 h. This preparation procedure yielded a terrace width of about 400 nm. The STM is specially designed to follow the entire film growth of the same region, providing a great accuracy in calibrating the coverage. The details of the STM and the coverage calibration technique are described elsewhere.[8,14] Nickel films were prepared from a nickel wire (purity 99.999%) heated by *e*-beam bombardment, with the pressure increasing up to 3×10^{-8} Pa during deposition. Carbon and oxygen contaminations were below 1.0 at. % as checked by AES. The Ni vapor beam intercepts the room-temperature (300±5 K) Cu substrate at an angle of 15° to the substrate surface. During deposition the STM tip is ~1 μm withdrawn from the sample surface in order not to shadow the Ni beam incident on the substrate. The deposition rate was kept constant at around 0.8 ML/min. All the STM images were taken in a constant-current mode (0.1 to 0.2 nA), with a positive bias on the sample of typically around 900 mV.

III. MORPHOLOGY OF THE Ni/Cu(100) FILM

Figure 1 demonstrates a nearly perfect two-dimensional growth of fcc Ni on Cu(100) in the submono-

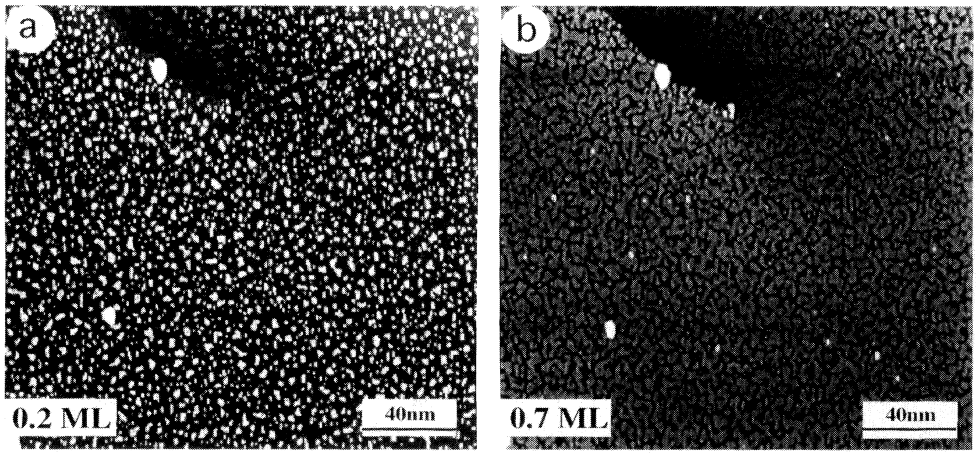

FIG. 1. STM images of initially grown Ni/Cu(100) films. (a) 0.2-ML coverage, the darker area is the substrate surface; (b) 0.7 ML. Note the minute amount of second-layer nuclei.

layer regime. Figure 1(a) shows the morphology of a 0.2-ML Ni film. Ni grows on Cu at a high nucleation density (about 7×10^4 islands/μm^2), with an average island size around 3 nm^2 at this coverage. Figure 1(b) shows the image of a 0.7-ML Ni film with the islands of the first layer becoming larger and approaching the stage at which the morphology percolation[9] of the first layer is completed. For a square lattice, assuming each site has the same probability to be occupied by an adatom, theoretical calculations[10] give a coverage of 0.59 ML as the percolation threshold value. For the particular system Ni/Cu(100), the best estimation of the first-layer percolation threshold thickness from our data is about 0.8 ML. The difference comes mainly from the nonuniformity of the island size distribution in real growth. Note that Fig. 1 only shows a few second-layer nuclei at a coverage as high as 0.7 ML.

Up to 3.4 ML, the film shows a very good layer-by-layer growth, as indicated in Fig. 2(a). The third layer (second darkest area) is almost complete whereas the number of nuclei of the fifth layer (brightest spots) is negligible. Although most of the islands of the fourth layer (second brightest islands) are of random shape, a few of them start to show a crystallographical orientation with their edges along [011] and [0$\bar{1}$1]. This trend becomes more pronounced at the higher coverage of 4.5 ML in Fig. 2(b), where most of the islands of the fifth layer (now second brightest islands) are nearly rectangular. Furthermore, at 4.5 ML the number of nuclei of the sixth layer (brightest spots) is more than that of the fifth layer for 3.4 ML. The height of the islands of both films is shown by the cross sections of the marked lines in the upper right corners. An interesting phenomenon is that the islands of the fourth layer in Fig. 2(a) are in almost the same positions as those of the fifth layer in Fig. 2(b). This "memory" phenomenon indicates a transition of the growth mode from layer-by-layer to multilayer growth, which will be discussed below.

Figure 3(a) shows that at a higher thickness of 5.6 ML, not only the islands of the sixth layer (second brightest islands) but also those of the seventh layer (brightest islands) are of rectangular shape. The islands of the seventh layer cover 9% of the whole area, which is still far less than that covered by the islands of the sixth layer (57% of the total area). The cross section of the marked line is plotted in the upper right of the image, showing the coexistence of monolayer and bilayer islands. At 7.1 ML [Fig. 3(b)], the total coverage with islands of the seventh (third brightest islands) and eighth layers (second brightest islands) is 75% and 35% of the whole area, re-

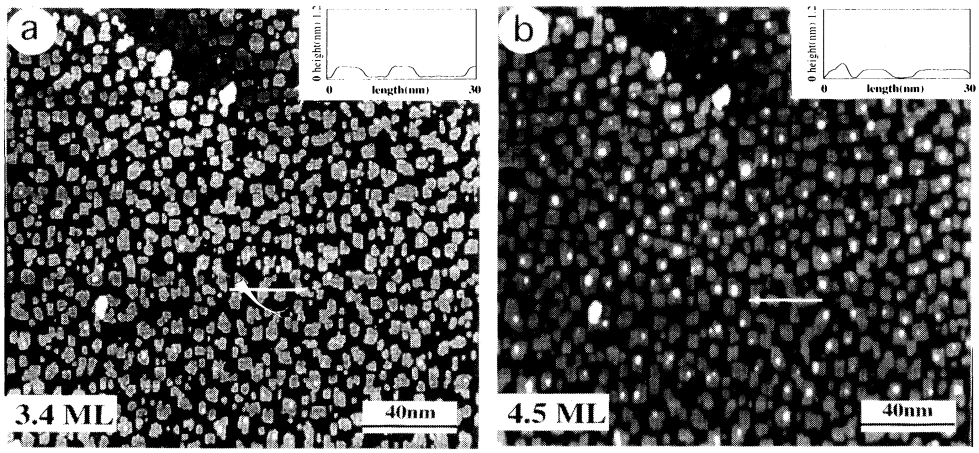

FIG. 2. STM images of (a) 3.4 ML and (b) 4.5 ML Ni/Cu(100) films. At 3.4 ML, the third layer is almost completed with hardly any fifth-layer nuclei forming. At 4.5 ML, the fourth layer is slightly less completed than the third one at 3.4 ML, with a few sixth-layer nuclei appearing on the surface. Note that at 3.4 ML only a few island edges are in the [011] and [0$\bar{1}$1] directions, which is more pronounced at 4.5 ML.

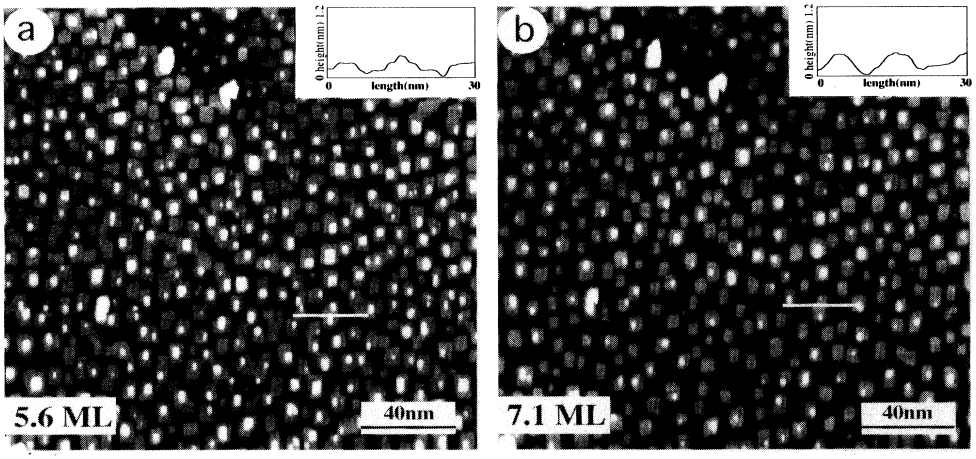

FIG. 3. STM images of (a) 5.6-ML and (b) 7.1-ML Ni/Cu(100) films. At 5.6 ML, the fifth layer is at 95% closed, with a considerable amount of seventh-layer islands (9% of the whole area) present. At 7.1 ML, the layer filling of the sixth (darkest), seventh (second darkest), eighth (second brightest), and ninth (brightest) layers are 97%, 76%, 34%, and 3%, respectively.

spectively. Most of the islands visible on the surface are bilayer islands as the marked line profile in the upper right of the image shows. The islands of the 7.1-ML film can thus be regarded as three-dimensional (3D) platelike islands of rectangular shape.

These 3d platelike islands gradually grow in size and height with increasing film thickness: starting from about 55 nm^2 and 0.4 nm at 7.1 ML, they rise up to 80 nm^2 and 1 nm, respectively, at 16.9 ML. Besides these changes in island size and height, no other distinct changes of the film morphology have been detected between 7.1 and 23 ML (23 ML is the largest thickness studied). The STM height measurements taken from all the films in this thickness region indicate that there is no change for the interplanar distance between the first layer (topmost layer) and the second layer within the measuring accuracy (±0.1 Å). Figure 4 presents the film morphology for 16.9 ML (a) and 20.3 ML (b), respectively. Note that the cross sections of the 3D islands shown in the upper right look like columnar islands, which is only due to the extremely exaggerated vertical scale in these STM images. Figure 5 presents the schematic cross sections of the 3D islands for 7 and 17 ML on a realistic scale. At 17 ML, the lateral dimensions of the islands are actually ten times larger than their height.

IV. DETERMINATION OF GROWTH MODE AND STRUCTURAL PROPERTIES

Now we turn to discuss the growth mode of this system. For determining the film growth mode, a common way is to look for reflection high-energy electron diffraction (RHEED) or medium energy electron diffraction (MEED) intensity oscillations with coverage. It is a real-time growth diagnostic and very convenient to do experimentally. But sometimes a film with morphology far away from layer-by-layer growth can also produce intensity oscillations with increasing coverages, making it difficult to judge the real growth mode. In the following we present the STM data of surface mean roughness (it has a close relation to RHEED or MEED Intensity as described below) and layer distribution with increasing coverages.

In Fig. 6, the surface mean roughness R is plotted as a function of film thickness. Here, the surface mean roughness is defined by the average distance from the surface to a reference center plane. It is calculated by

$$R = \frac{1}{L_x L_y} \int_0^{L_y} \int_0^{L_x} f(x,y)\,dx\,dy \ ,$$

where $f(x,y)$ is the distance from the surface to a refer-

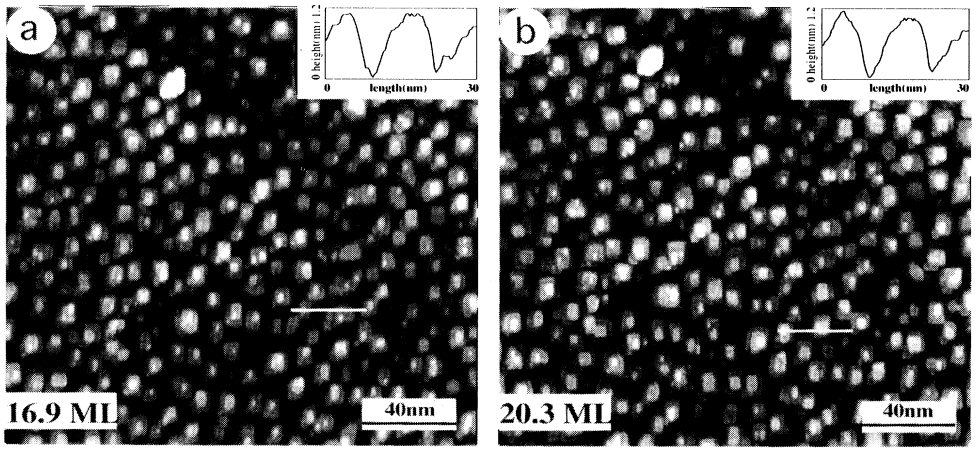

FIG. 4. STM images of (a) 16.9-ML and (b) 20.3-ML Ni/Cu(100) films. The 3D rectangular islands at these coverages are higher than those at lower coverages. Marked line profiles are shown in both images, indicating that the 3D islands are about 1 nm high in both films.

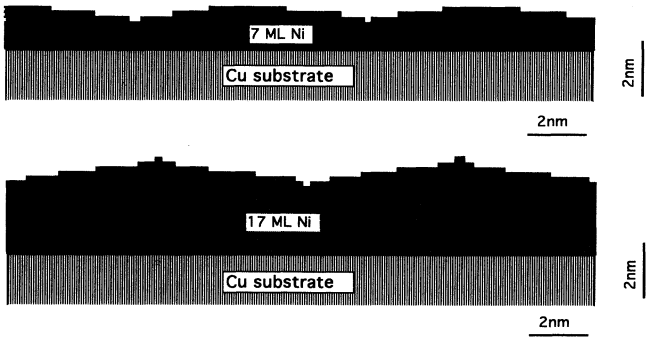

FIG. 5. Schematic cross sections of 7- and 17-ML Ni/Cu(100) films. Note that at 17 ML the lateral dimension of the 3D platelike islands is 10 times larger than their height.

ence center plane, and L_x, L_y are the dimensions of the surface. A larger mean roughness corresponds to a morphology that has more layers simultaneously exposed to the surface or a larger area of those layers that is farther away from the center plane. The standard deviation of the height values of all the points within the scanning area (rms) was also plotted out (not shown here) with increasing coverages, and is very consistent with Fig. 6. According to the characteristic features of this surface roughness curve, two growth regions can be identified. As shown in the plot, in region I from 0 to 6 ML the surface roughness is oscillating with increasing coverage with a periodicity of 1 ML. The lowest roughness value for each oscillation corresponds to an integral number of coverage, which is typical of the surface roughness if the film is growing in a near layer-by-layer mode. The oscillations below 4 ML are apparently stronger than those two between 4 and 6 ML, indicating that a multilayer growth starts at a thickness of 4 ML. This is quite consistent with the "memory" phenomenon mentioned before, because the "memory" of the islands can only result from the fact that the islands of the fifth layer already start growing before those of the fourth layer get coalescing. Moreover, since the roughness data obtained from the STM images are closely related to the electron-diffraction intensity,[11,12] one would also expect a similar behavior of the MEED or RHEED intensity in this region. Above 6 ML in region II, the roughness simply increases with coverage, indicating a dominant multilayer growth.

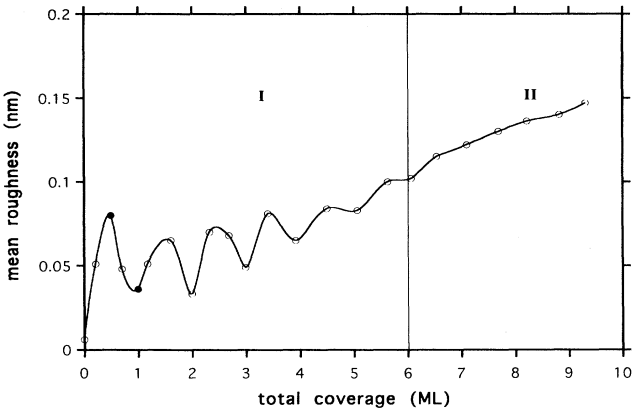

FIG. 6. Surface mean roughness plotted vs total coverage for the Ni/Cu(100) system. For 0–6 ML, the regular oscillations with a periodicity of 1 ML reflect a nearly layer-by-layer growth in region I. Above 6 ML, the roughness simply increases with increasing coverage owing to the increasing height of the 3D islands. The two full dots are from a different experiment. The full line is a guide to the eye.

The layer distribution versus the total coverage is plotted in Fig. 7. This graph gives more detailed information about the film growth mode than Fig. 6 does. Figure 7 demonstrates that at the coverage of only 0.7 ML the second-layer growth starts. At a coverage of 1 ML 90% of the first layer is completed while the remaining 10% appears as second-layer islands. This two-layer growth is the main growth mode in the thickness range between 0.7 and 3.5 ML. At 2 ML 95% of the second layer is completed, whereas at 3 ML 90% of the third layer is accomplished. In reality, in the thickness range of 0–3.5 ML, the film is showing a good layer-by-layer growth with the island shape being irregular in this region. Above 3.5 ML the film growth is more complicated with the island shape becoming rectangular. Pronouncedly rectangular islands were observed to form at a coverage of about 4 ML. In the 3.5–6-ML region, the film grows in a three-layer growth mode, and above 6 ML the film is growing by even four layers at the same time. The formation of platelike 3D islands of rectangular shape is most obvious at 7.1 ML [Fig. 3(b)]: the islands are about 0.4 nm high and 7 to 8 nm wide, with their edges along [011] and [0$\bar{1}$1].

Combining the information of film morphology (Figs. 1–4), roughness (Fig. 6), and layer distribution (Fig. 7) enables two growth regions of Ni/Cu(100) to be defined: region I covers the range of 0–6 ML, where the film

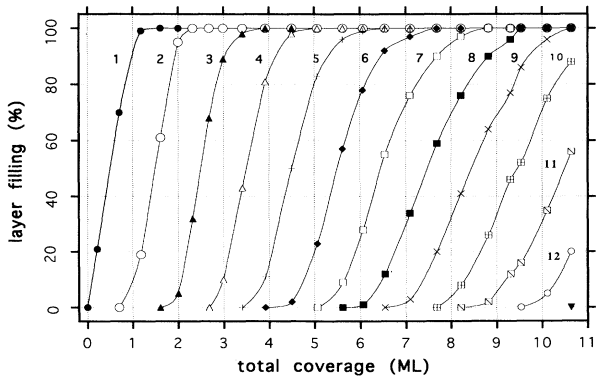

FIG. 7. Layer coverage as a function of total coverages for the Ni/Cu(100) film. This plot gives information about the layer distribution at a certain total coverage. Numbers 1–12 refer to the curves of the first to the twelfth layer.

shows a nearly layer-by-layer growth. In this region, the film is in a two-layer growth mode between 0 and 3.5 ML with irregularly shaped islands, and from 3.5 to 6 ML the film growth is in a transition region from layer-by-layer growth to multilayer growth; In region II above 6 ML, the film grows in a multilayer mode by forming rectangular platelike 3D islands.

A striking feature in Figs. 3 and 4 is the formation of fairly uniform rectangularly shaped islands. The shape and orientation of the islands in this system are determined by energy and symmetry: step edges along [011] form the most stable close-packed (111) microfacets; the fourfold symmetry of fcc (100) lattices results in identical stability of the four possible step orientations, explaining the near square shape of the islands. In the STM images most of the islands appear to be slightly distorted from square shape in the same direction, this is mainly due to a small thermal drift during the experiments. In fact, previous STM studies of nucleation and growth on (100) faces of fcc Ni,[13] annealed fcc Fe,[14] and bcc Fe (Ref. 15) have also shown the rectangular shape of the islands, which is just the expected equilibrium shape.[16,17] Thus, we can conclude that above 4 ML in our system island restructuring is faster than island growth, and [011] and [0$\bar{1}$1] are the preferential directions of the island edge atoms arranged on the surface. The question arises as to why the islands show a distinct rectangular shape only at thicknesses above 4 ML, but not below, i.e., at thicknesses above 2 ML, where usually the substrate influence on the film electronic structure is very weak. Concerning this question, we first point out that the thickness (4 ML) at which the rectangular islands start to appear is also the onset of multilayer growth. This is not simply an accidental coincidence. The island shape in this system is determined by two competing processes: (1) the diffusion of the island step-edge atoms along the edges to align in the [011] direction shape the islands rectangularly; (2) the diffusion of the atoms on top of the islands across the edges, together with islands coalescence tend to make the islands randomly shaped. As mentioned above, at the thickness (4 ML) of the beginning formation of rectangularly shaped islands, the film changes from layer-by-layer growth to multilayer growth. The latter may be due to an enhanced island step edge barrier ("Schwoebel barrier"). The enhanced Schwoebel barrier prevents the atoms on top of the existing islands from passing the island edges, which in return also suppresses the coalescence of the islands. This effect makes the rectangular shaping process overcome the random shaping process, resulting in the formation of rectangular islands above 4 ML. The driving mechanism of the increasing "Schwoebel barrier" is not yet clear: the influence of the substrate on the film electronic structure could play a role, but this effect is usually expected to be very weak for films thicker than 2 ML; 2.5% tensile strain might be very important for the change of the "Schwoebel barrier," and in fact the misfit strain does considerably affect the diffusion barrier in an Ag/Pt(111) system.[18] The effect coming from the strain could be dominant at higher thicknesses (>4 ML) where the influence of the substrate electronic structure presumably becomes negligible. Experimental data and theoretical simulations of the electronic structure and the strain-dependent diffusion barrier of thick Ni films (~ 4 ML) are necessary to elucidate respective details.

V. ANNEALING EFFECT ON THE MORPHOLOGY AND MAGNETIC ANISOTROPY

As mentioned, the magnetic easy axis is in-plane up to 7 ML, and goes out-of-plane for higher thicknesses above 7 ML. As shown in Fig. 3, the well-defined 3D platelike islands start to form also at about 7 ML. A question immediately arises: Is there any relationship between the formation of 3D platelike islands and the transition of the magnetic anisotropy which takes place at a similar thickness of 7 ML?[3–5]

To address this question, the most direct way is to modify the morphology of the films that are thicker than 7 ML and to check whether this morphology modification will give rise to a corresponding change of the magnetic anisotropy. Common methods for modifying film morphology include variable substrate temperature deposition, surfactant assisted growth, and annealing. Since it has been reported that Ni on Cu is thermally stable against interdiffusion to cycling temperatures up to 490 K,[19] we decided to use annealing to serve our purpose. Annealing is usually applied to improve the film quality, such as healing the defects, prolonging the layer-by-layer growth region, etc. On the other hand, in systems such as Co/Cu(100) (Ref. 20) and Fe/Cu(100),[14] microscopic pinholes form upon annealing, serving as channels for the substrate copper to diffuse to the top of the film via surface diffusion. Ni/Cu(100), however, does not show such a surface diffusion upon annealing. Figure 8 shows the film morphology of 3.1-ML Ni/Cu(100) before (a) and after (b) annealing at 450 K for 10 min. As described in Sec. III, at a thickness of 3.1 ML the film is in a good layer-by-layer growth regime. Figure 8(a) shows that three layers appear simultaneously on the surface: the second (darkest), the third, and the fourth (brightest) layer. However, after annealing the film shows a morphology like that of a perfect layer-by-layer growth. In Fig. 8(b), the third layer is 100% complete, and the bright islands are fourth-layer islands as shown in the line profile in the upper right corner. After annealing the surface mean roughness decreased by more than a factor of 2, from 0.056 to 0.020 nm. No microscopic pinholes formed upon annealing, with the AES peak-to-peak ratio of Ni(848)/Cu(920) only slightly changing, indicating there was no significant interdiffusion during annealing.

Annealing thicker films at 450 K also considerably smooths the film surface. Figure 9 shows the annealing effect on a 10.2-ML film. Before annealing [Fig. 9(a)], the film surface exhibits five layers simultaneously: the eighth, ninth, tenth, eleventh, and twelfth ones (the brightest islands are those of the twelfth layer). After annealing at 450 K for 10 min [Fig. 9(b)], the film is much smoother, revealing only three layers on the surface. The darkest areas are openings of the ninth layer, the brightest ones are of the eleventh layer. The line profile of the marked white line is drawn in the upper right corner,

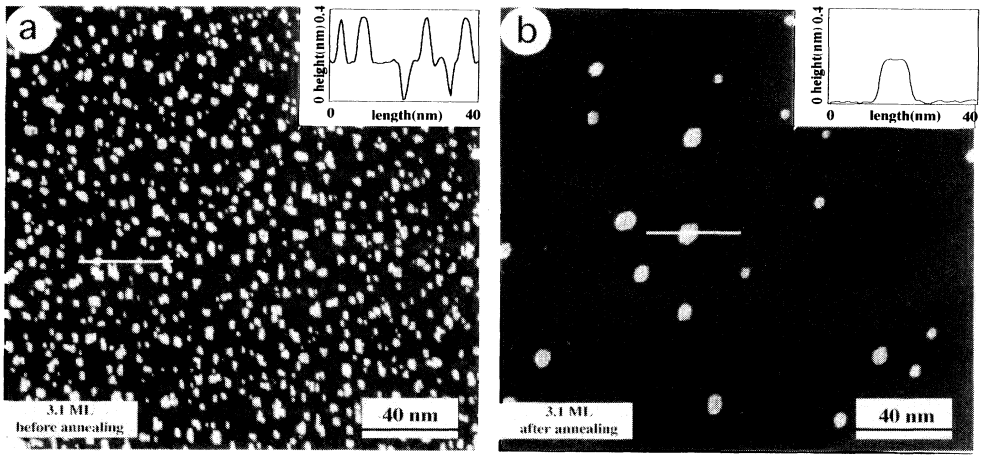

FIG. 8. Annealing effect (450 K, 10 min) on the morphology of a 3.1-ML Ni/Cu(100) film. (a) before annealing there are 3 layers (second, third, and fourth) evident on the surface, (b) after annealing the third layer is at 100% completed.

showing the relative height of the surface features. The mean film roughness drops from 0.155 nm before annealing [Fig. 9(a)] to 0.063 nm after annealing [Fig. 9(b)]. Note that the mean roughness of the 10.2-ML annealed film is almost the same as the average mean roughness in the near layer-by-layer growth regime (Fig. 6). AES data show that after annealing the Ni(848)/Cu(920) ratio increases by about 10%, which is mainly due to the completion of the lower layers after annealing.

Since we find that annealing significantly smooths the film surface, if the multilayer growth was really responsible for the perpendicular anisotropy, then the perpendicular magnetization of the film should be considerably reduced or even disappear after annealing. However, our MOKE study of a 10.2-ML-thick film shows that after annealing the magnetization remains perpendicular, decreasing by less than 15%. Substracting the reduction of magnetization from slight contamination owing to annealing, we can conclude that the annealing effect on the perpendicular magnetization is negligible. This implies that the multilayer growth is not responsible for the switch from in-plane to perpendicular magnetization at larger film thicknesses. A detailed study of the magnetism of this system will be reported in a forthcoming paper.

VI. SUMMARY

In summary, we have demonstrated that STM can provide valuable information about the growth mode and structural properties of ultrathin films if used to follow the film growth in a particular region. A good layer-by-layer growth is observed up to 3.5 ML, and above 4 ML well-defined-rectangularly shaped islands start to form. Distinct multilayer growth of the film starts from 6 ML on. The 3D platelike islands show a rectangular shape

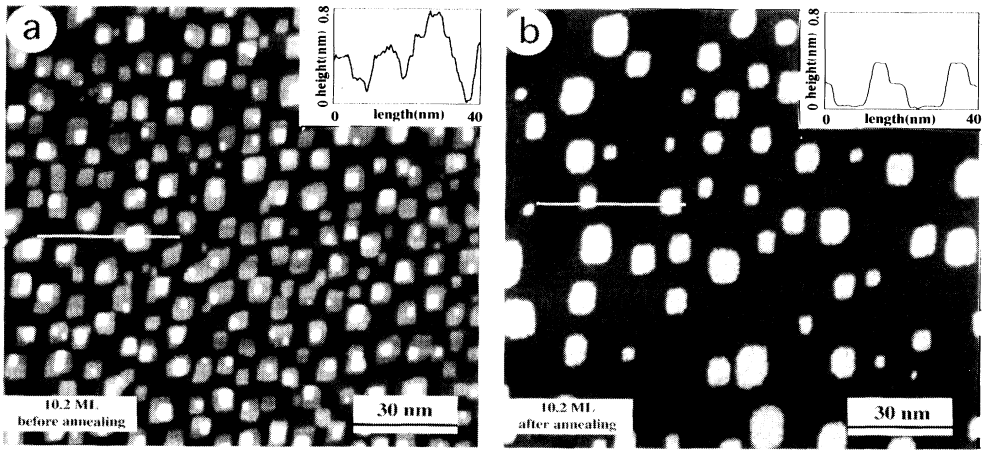

FIG. 9. Annealing effect (450 K, 10 min) on the morphology of a 10.2-ML Ni/Cu(100) film. (a) before annealing there are 5 layers (eighth to twelfth) visible, (b) after annealing only the ninth, tenth, and eleventh layers are exposed, with the line profile of the marked white line shown in the upper right.

with their edges in the [011] and [0$\bar{1}$1] directions, indicating that the [011] direction has the lowest-energy barrier for surface diffusion. Annealing the film at 450 K smooths the film surface without any significant substrate interdiffusion. The fact that the perpendicular magnetization remains almost constant upon annealing indicates that the 3D growth in this system does not play a key role in the perpendicular magnetic anisotropy.

ACKNOWLEDGMENT

The authors would like to thank M. Klaua for helpful discussions.

*Author to whom correspondence should be addressed.

[1]H. J. Elmers *et al.*, Phys. Rev. Lett. **73**, 898 (1994).

[2]J. Giergiel, J. Shen, J. Woltersdorf, A. Kirilyuk, and J. Kirschner, Phys. Rev. B **52**, 8528 (1995).

[3]F. Huang, M. T. Kief, G. J. Mankey, and R. F. Willis, Phys. Rev. B **49**, 3962 (1994).

[4]W. L. O'Brien and B. P. Tonner, Phys. Rev. B **49**, 15 370 (1994).

[5]B. Schultz and K. Baberschke, Phys. Rev. B **50**, 13 467 (1994).

[6]M. A. Abu-Joudeh, B. M. Davies, and P. A. Montano, Surf. Sci. **171**, 331 (1986).

[7]J. Zhang, Z.-L. Han, and S. Varma, Surf. Sci. **298**, 351 (1993).

[8]A. Schmid and J. Kirschner, J. Vac. Sci. Technol. B **49**, 649 (1991).

[9]Percolation as mathematically defined (finite probability of an infinite path) cannot be tested in our system. Instead, we use an operational definition—95% of islands of a given height must be interconnected on a representative 25×25-nm^2 area before they are considered percolated.

[10]F. Yonezawa, S. Sakamoto, and M. Hori, Phys. Rev. B **40**, 636 (1989).

[11]D. D. Chambliss and K. E. Johnson, Surf. Sci. **313**, 215 (1994).

[12]C. M. Schneider, A. K. Schmid, P. Schuster, H. P. Oepen, and J. Kirschner, in *Magnetism and Structure in Systems of Reduced Dimensions,* edited by R. F. C. Farrow *et al.* (Plenum, New York, 1993), p. 453.

[13]E. Kopatzki, S. Günther, W. Nichtl-Pecher, and R. J. Behm, Surf. Sci. **284**, 154 (1993).

[14]J. Shen, J. Giergiel, A. K. Schmid, and J. Kirschner, Surf. Sci. **328**, 32 (1995).

[15]J. A. Stroscio, D. T. Pierce, and R. A. Dragoset, Phys. Rev. Lett. **70**, 3615 (1993).

[16]A. Voter, Proc. SPIE **821**, 214 (1987).

[17]W. K. Burton, N. Cabrera, and F. C. Frank, Philos. Trans. R. Soc. London Ser. A **243**, 299 (1951).

[18]H. Brune, K. Bromann, H. Roder, and K. Kern (private communication).

[19]Y. Chen, S. T. Tong, J. S. Kim, M. H. Mohamed, and L. L. Kesmodel, Phys. Rev. B **43**, 6788 (1991); M. H. Mohamed, J. S. Kim, and L. L. Kesmodel, *ibid.* **40**, 1305 (1989).

[20]A. K. Schmid, D. Atlan, H. Itoh, B. Heinrich, T. Ichinokawa, and J. Kirschner, Phys. Rev. B **48**, 2855 (1993).

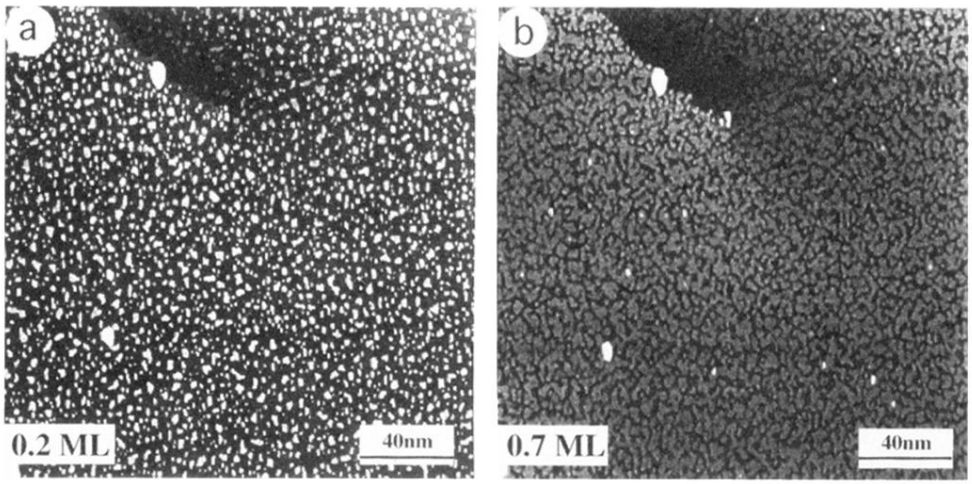

FIG. 1. STM images of initially grown Ni/Cu(100) films. (a) 0.2-ML coverage, the darker area is the substrate surface; (b) 0.7 ML. Note the minute amount of second-layer nuclei.

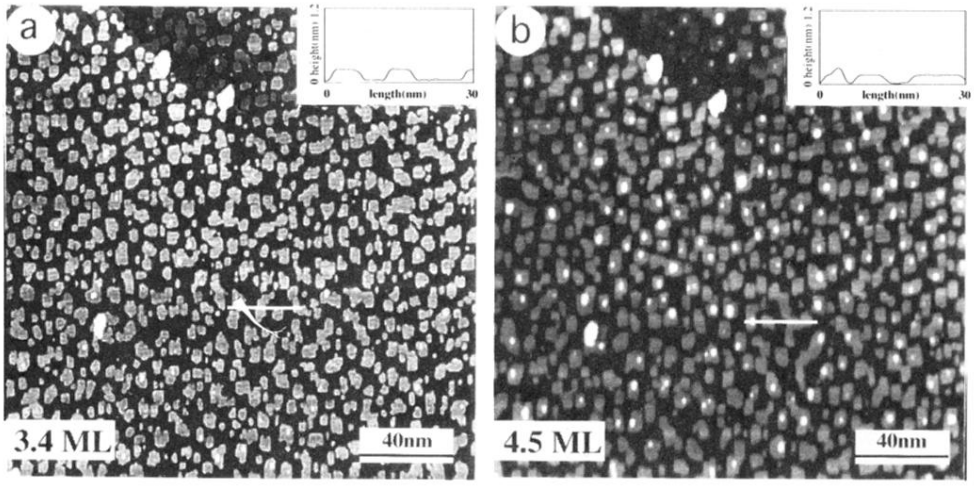

FIG. 2. STM images of (a) 3.4 ML and (b) 4.5 ML Ni/Cu(100) films. At 3.4 ML, the third layer is almost completed with hardly any fifth-layer nuclei forming. At 4.5 ML, the fourth layer is slightly less completed than the third one at 3.4 ML, with a few sixth-layer nuclei appearing on the surface. Note that at 3.4 ML only a few island edges are in the [011] and [$0\bar{1}1$] directions, which is more pronounced at 4.5 ML.

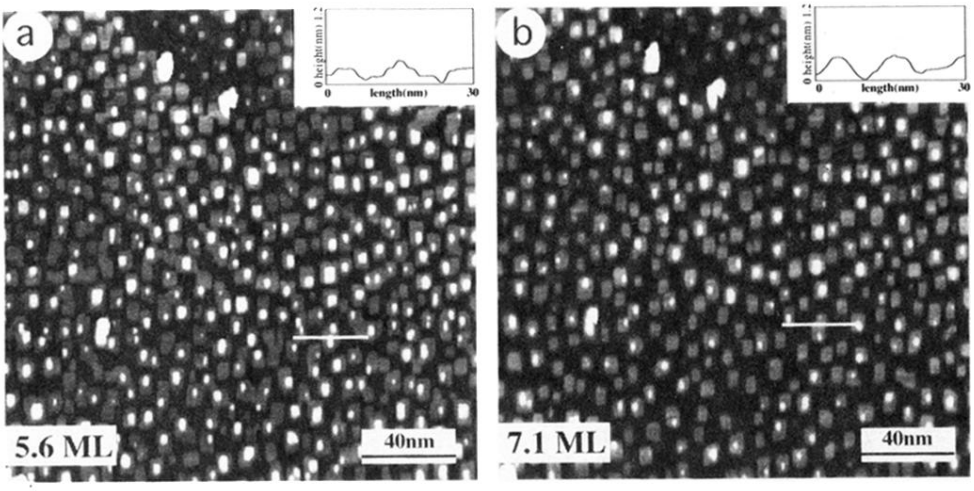

FIG. 3. STM images of (a) 5.6-ML and (b) 7.1-ML Ni/Cu(100) films. At 5.6 ML, the fifth layer is at 95% closed, with a considerable amount of seventh-layer islands (9% of the whole area) present. At 7.1 ML, the layer filling of the sixth (darkest), seventh (second darkest), eighth (second brightest), and ninth (brightest) layers are 97%, 76%, 34%, and 3%, respectively.

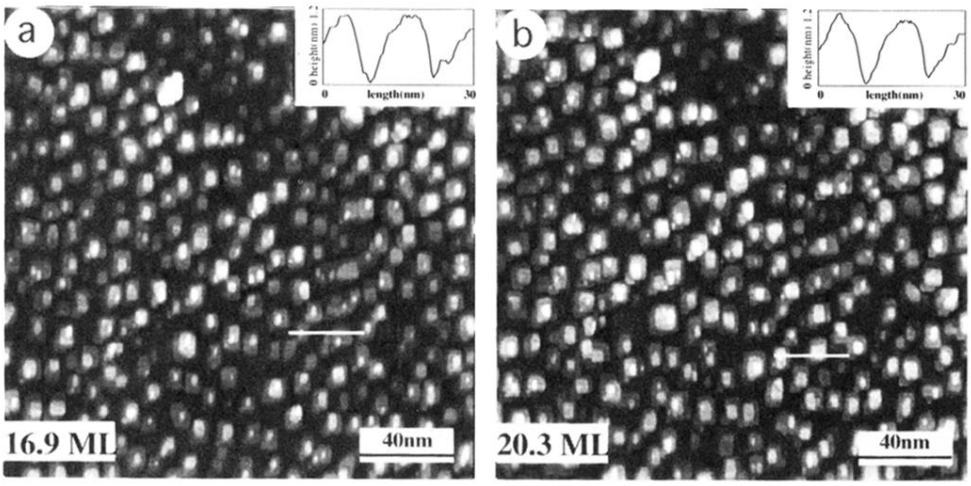

FIG. 4. STM images of (a) 16.9-ML and (b) 20.3-ML Ni/Cu(100) films. The 3D rectangular islands at these coverages are higher than those at lower coverages. Marked line profiles are shown in both images, indicating that the 3D islands are about 1 nm high in both films.

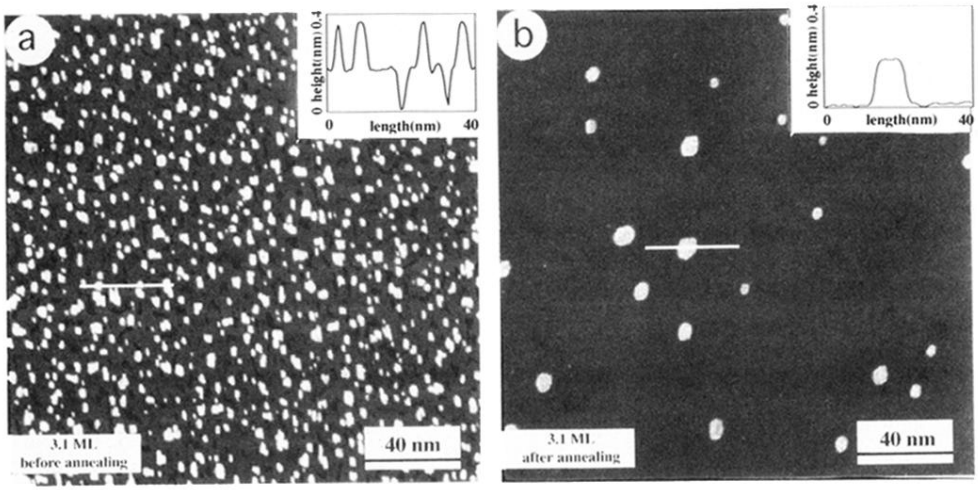

FIG. 8. Annealing effect (450 K, 10 min) on the morphology of a 3.1-ML Ni/Cu(100) film. (a) before annealing there are 3 layers (second, third, and fourth) evident on the surface, (b) after annealing the third layer is at 100% completed.

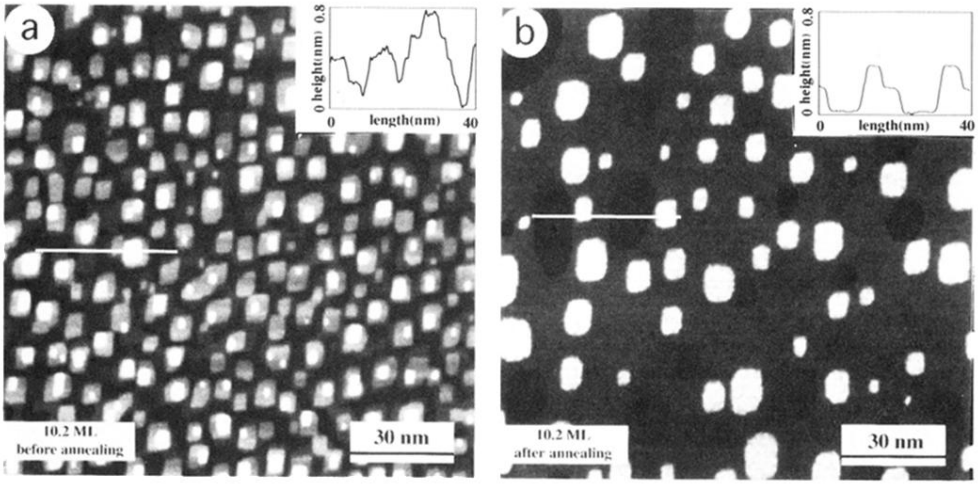

FIG. 9. Annealing effect (450 K, 10 min) on the morphology of a 10.2-ML Ni/Cu(100) film. (a) before annealing there are 5 layers (eighth to twelfth) visible, (b) after annealing only the ninth, tenth, and eleventh layers are exposed, with the line profile of the marked white line shown in the upper right.